

# CURES OF INSTABILITIES

*D. Boussard*

CERN, Geneva, Switzerland

## **Abstract**

Careful design of machine elements, in particular the RF cavities, may be sufficient to avoid beam instabilities in circular accelerators, with the help of natural synchrotron radiation damping ( $e^+e^-$  machines) or Landau damping in the case of hadron beams. If this is not sufficient feedback systems, transverse or longitudinal, have to be employed. A review of the various techniques in use against beam instabilities induced by long-range wake fields is given in this paper.

## **1. INTRODUCTION**

Accelerators are often plagued by various sorts of instabilities which limit their maximum beam currents. In the case of circular machines, which we consider here, one can distinguish between strong, turbulent instabilities driven by short range wake fields (the microwave instability, the transverse mode coupling instability are good examples) and weak multiturn instabilities which are, in most cases, due to long range fields. Against turbulent instabilities one can only consider "preventive" measures aimed at raising the threshold beam currents (the notable exception being the use of reactive feedback against mode coupling transverse instabilities, which we will not discuss here). Preventive measures comprise the minimization of the broad band impedance of the vacuum chamber by screening any abrupt cross section change (bellows, vacuum manifolds, etc...) and by a proper design of protruding elements like pick up and clearing electrodes.

Strong, turbulent instabilities must be avoided by a careful choice of parameters for any new machine design (the same is true also for instabilities with high, within bunch mode, numbers which are difficult to damp by active feedback).

In the following we shall concentrate on "slow" instabilities, for which effective "countermeasures" can be engineered.

## **2. DAMPING OF NARROW BAND IMPEDANCES**

Most slow instabilities are driven by long-memory, narrow-band impedances (this is not the case however for the head-tail instability, transverse or longitudinal). In many cases, especially for  $e^+e^-$  machines which require a large RF voltage, the major source of narrow-band impedances are the higher-order modes (HOM's) of the accelerating cavities.

The problem here is to damp as much as possible all HOM's, without affecting the fundamental, accelerating mode. Higher-order mode dampers are essentially high-pass devices whose corner frequency is located above the fundamental and below the first HOM frequencies. To improve the rejection of the accelerating mode a notch filter is often combined with the HOM coupler. In this case one must pay attention to the high RF currents at the RF frequency which flow in the notch filter elements. A simple form of high-pass filter is a waveguide with a cut off frequency above the fundamental resonance of the cavity. The position of the waveguide(s) in the cavity can be optimized such as to couple to as many HOM's as possible [1]. Figures 1 and 2 shows an example of such a design with several waveguides attached to a copper cavity. Note the long tapers on either side of the cavity itself to minimize the contribution of the RF cavity to the broad band impedance of the ring (DAFNE) [2]. The waveguides can also be the vacuum chamber itself, as in Fig. 3, which

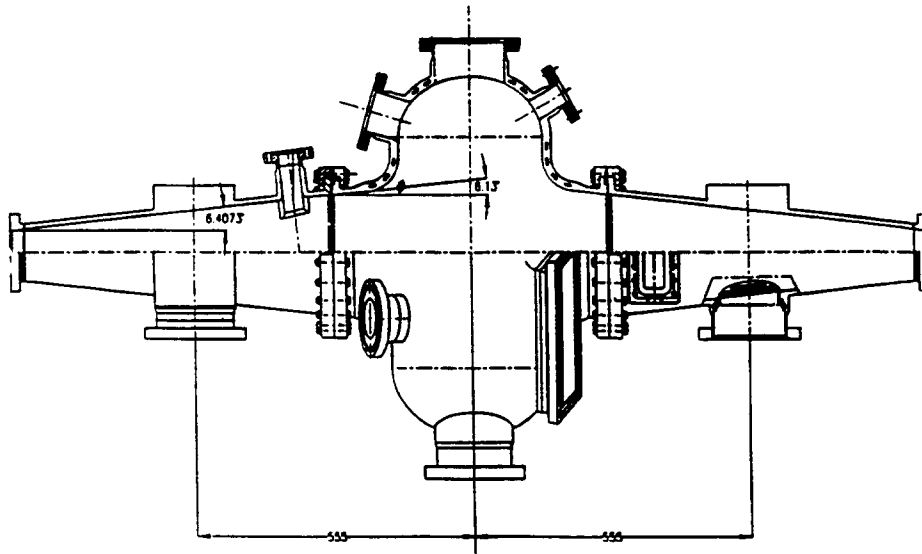


Fig. 1 Sketch of the DAFNE cavity with waveguide ports for HOM damping

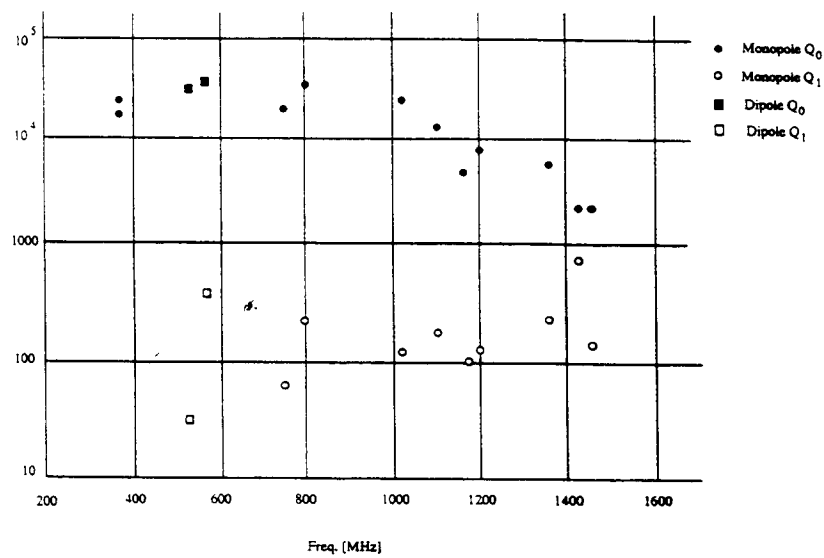


Fig. 2 Undamped and damped Q values of the lowest HOM's of the DAFNE cavity

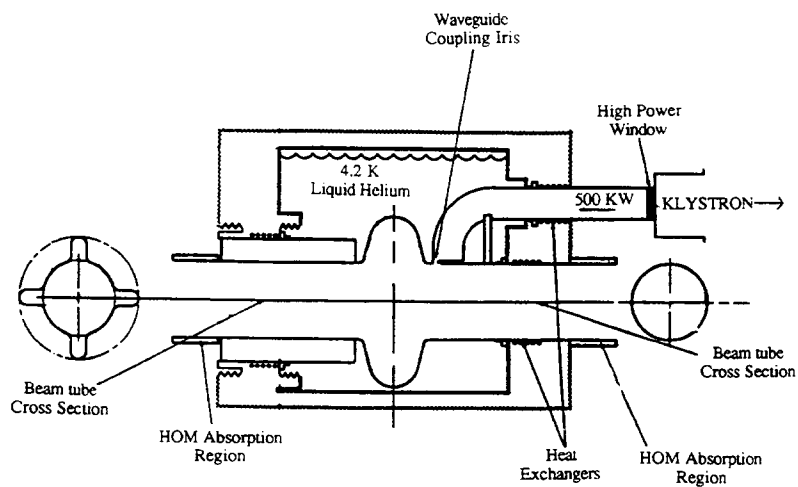


Fig. 3 Sketch of the CESR B superconducting cavity

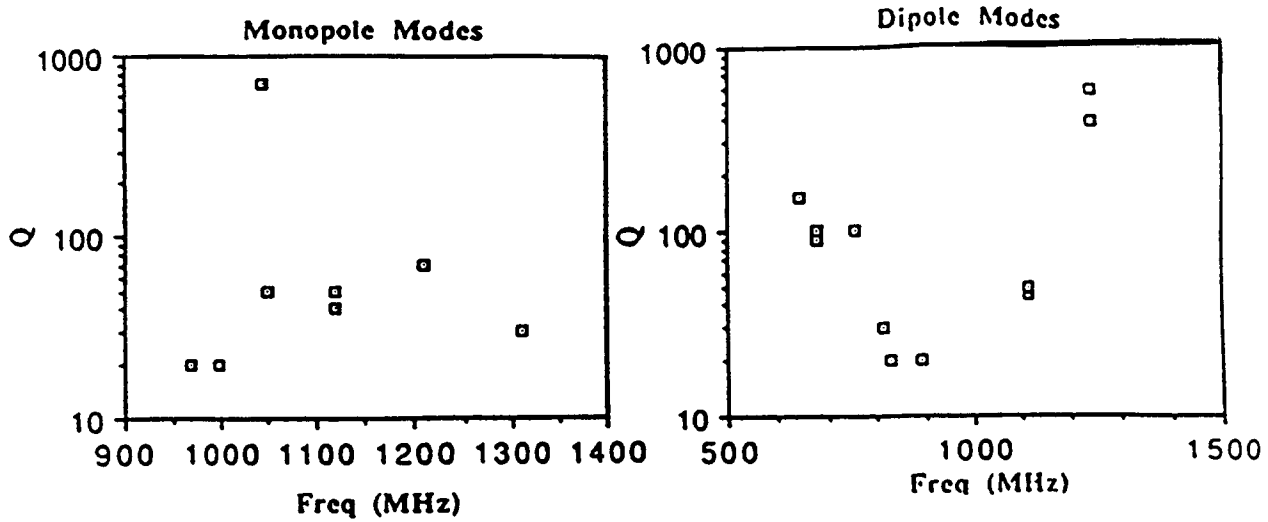


Fig. 4 Damped Q values for the CESRB cavity

shows the CESRB superconducting cavity design [3]. The so-called "fluted" vacuum chamber shape gives a lower cut off frequency as compared to a cylindrical waveguide and let also the first two transverse modes propagate outside the cryostat. In this case damping of the HOM resonators is accomplished with lossy material (ferrites) inside the vacuum chamber. With conventional waveguides, the damping elements can be inside vacuum, as waveguide terminations, in the case of small power dissipation (CEBAF, for instance). They can also be outside vacuum in coaxial form, if broad-band waveguide-coaxial transitions and coaxial vacuum feedthroughs are employed [4]. Figures 2 and 4 show the results of HOM damping for the two previous examples and illustrate the present state of the art ( $Q_{\text{ext}}$  of the order of 100 or less).

Many other damping techniques are in use, or have been proposed, notably tuned antennas to damp a particular mode in the cavity. For low-frequency cavities damping elements having a high pass characteristic can be inserted in "series" with the accelerating gap to provide damping of all longitudinal modes [5].

### 3. DAMPING MECHANISMS AND THRESHOLDS

#### 3.1 Synchrotron radiation

In electron or positron machines, synchrotron radiation provides a natural damping to individual particle oscillations, and thus to any collective bunch motion. The instability threshold is given simply by the condition:

$$\Delta\omega_{mn} < 1/\tau_r$$

where  $\Delta\omega_{mn}$  is the imaginary part of the frequency shift due to the instability and  $\tau_r$  the radiation damping time, either the energy damping time if one considers longitudinal instabilities or the horizontal, vertical damping times in the transverse case.

For the longitudinal case, Table I gives typical numbers for two very different machines (the small 500 MeV DAFNE ring, and the very large ring of LEP). Even in the latter case

where synchrotron radiation is very strong, natural damping of longitudinal oscillations is fairly weak ( $\Delta\omega_s / \omega_s \approx 10^{-3}$ ).

**Table 1**  
Some parameters of two very different machines

Machine	Revolution frequency $f_0$ (Hz)	Synchrotron time $Q_s$	Energy damping time $\tau_z$ (s)	Relative synchrotron frequency shift $\Delta\omega_s / \omega_s = 1 / \tau_r \omega_s$
DAFNE	3.07 10 <sup>6</sup>	0.0123	17.8 10 <sup>-3</sup>	2.32 10 <sup>-4</sup>
LEP (45 GeV)	11246	0.085	17.81 10 <sup>-3</sup>	9.3 10 <sup>-4</sup>

### 3.2 Landau damping

There is always a spread of individual particles' frequencies in a bunch population, which is due to, for instance the non-linearity of the restoring force. This is notably the case for the synchrotron oscillations with a sinusoidal RF voltage or in the case of transverse oscillations when octupolar fields are present.

The obvious consequence of a spread of oscillation frequencies is that any coherent motion will ultimately result in a macroscopic increase of the beam emittance, a process often called filamentation. This has naturally a self stabilizing effect on any instability as the coherent oscillation resulting from the instability is transformed into an emittance increase which usually corresponds to a larger frequency spread. Ultimately the beam may become stable when the frequency spread is large enough for Landau damping to be effective.

Unfortunately this is a process difficult to predict (competition between instability growth and filamentation), it very often leads to unacceptable losses and in any case produces beam blow-up which may be undesirable. One has to mention, however, that many machines operate in this way; this is the case if beam losses are small enough and if emittance blow-up is not of great concern.

The spread of individual particles' oscillation frequencies also prevents instabilities developing below a certain threshold, a process improperly called Landau "damping". There is no damping as such, as in the case of synchrotron radiation, rather the instability cannot grow from initially microscopic disturbances. The threshold below which the beam stays stable depends on the details of the distribution of individual frequencies and the type of instability (mode number, etc...).

In the longitudinal plane, for the dipole mode and a smooth distribution, the approximate Landau damping criterion can be written [6]:

$$\frac{|\Delta\omega_s|}{\omega_s} < \frac{1}{4} \frac{s}{\omega_s} \quad (1)$$

where  $|\Delta\omega_s|$  is the magnitude of the instability frequency shift, and  $s/\omega_s$  the relative synchrotron frequency spread inside the bunch.

For a non-accelerating bucket ( $\phi_s = 0$ ) one has, for a sinusoidal RF voltage:

$$\frac{s}{\omega_s} \approx \frac{\pi^2}{16} \left( \frac{\text{bunch length}}{\text{RF period}} \right)^2 \quad (2)$$

Landau damping is especially efficient for long bunches, usually the case with protons or heavy particles, for which synchrotron radiation is non-existent. For non-accelerating buckets ( $\phi_s = 0$ ) a possible cure [7] of coupled bunch longitudinal instabilities is to reduce the RF voltage  $V$ ; this increases dramatically  $s/\omega_s$  when the beam edge approaches the separatrix. For a stationary bucket this method does not work because the instability growth rate  $(\Delta\omega_s)/\omega_s$ , proportional to  $1/V$ , increases faster than  $s/\omega_s$ .

An illustrative picture of Landau damping is given on Fig. 5 where the distribution of individual particles' oscillation frequencies is shown. For the dipole mode, the zero intensity coherent frequency  $\omega_c$  is located inside the distribution (in the case of the so-called waterbag model, with uniform particle density in phase space up to a limit amplitude, and zero beyond,  $\omega_c$  is just on the edge of the distribution). When the beam current is increased, the coherent frequency  $\omega_c$  is shifted by an amount  $\Delta\omega_c$ , usually complex. Landau damping is effective if the new value  $\omega'_c$  is still inside the initial distribution of incoherent frequencies. This is a condition similar to Eq. (1) except for the numerical factor which depends on the particular case of interest (mode number, type of distribution, type of impedance).

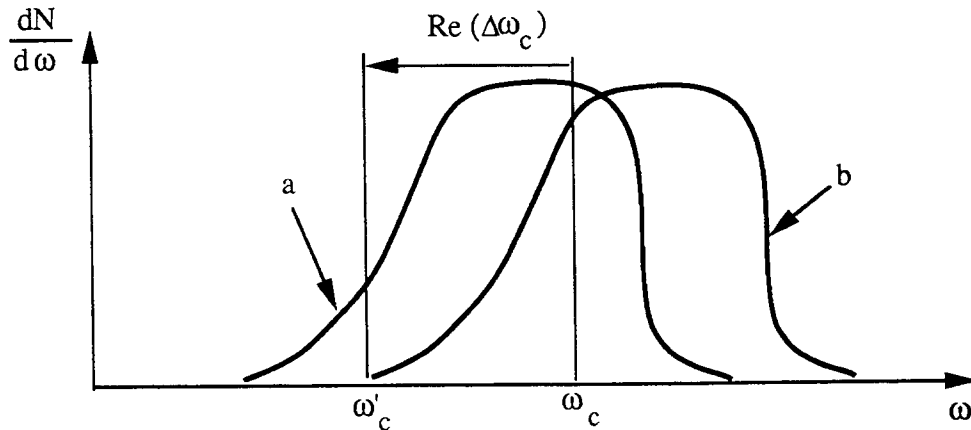


Fig. 5 An illustrative picture of Landau damping: a) without reactive broad band impedance, b) with reactive broad band impedance

This picture also illustrates the effect of the reactive part of the machine broad band impedance (space charge, inductive wall), which is to change the spectrum of incoherent frequencies (Fig. 5b). The coherent line  $\omega_c$  may or may not be displaced depending on the interaction considered. In particular, the frequency of the longitudinal dipole mode is not shifted when one considers the effect of the inductive wall impedance. In the new situation, illustrated in Fig. 5b, the instability line may fall outside the spectrum of incoherent frequencies, resulting in a complete loss of Landau "damping". One then observes coherent beam oscillations sustained for very long periods, much longer than would be anticipated from the spread of incoherent frequencies. In conclusion the effect of the broad band impedance, even though it does not produce beam instabilities in itself, may be to provoke a complete loss of Landau damping. The rule of thumb criterion for this to happen is when the frequency shift due to the broad-band impedance becomes comparable to the natural frequency spread in the zero intensity beam.

By making the restoring force highly non-linear one can considerably increase the natural frequency spread within the bunch. "Landau" cavities operating at a multiple of the RF frequency can be used for this purpose. The combination of RF voltages from the normal accelerating cavities and the "Landau" cavities can be such that the synchrotron frequency goes to zero at the bunch centre giving maximum synchrotron tune spread, and therefore maximum Landau "damping". It must be pointed out, however, that Landau cavities have been found not very effective when the bucket is already almost full, presumably because the tune spread which is already comparable to the synchrotron frequency does not change dramatically. The control of harmonic cavities, in the presence of strong beam loading, may also be difficult [8].

### 3.3 Bunch-to-bunch frequency splitting

The idea here is to reduce the coupling between bunches and hence the instability growth by making their unperturbed oscillation frequencies slightly different. This is reminiscent of Landau damping, although there we have a limited number of resonators (the number of bunches) with different frequencies. This makes computer simulation relatively easy unless the number of bunches is very large.

Indeed one observes a reduction of the growth rate or the suppression of the instability depending on the spread in oscillation frequencies, the frequency splitting pattern and the instability parameters. In all cases the stabilizing effect is weak; only instabilities with  $\Delta\omega_s / \omega_s \leq 0.01$  can be suppressed by this method.

In the transverse plane, betatron frequency splitting can be achieved with an RF quadrupole excited at a multiple of the revolution frequency. Synchrotron frequency splitting is obtained with RF cavities driven at  $p f_0$  ( $f_0$ : revolution frequency,  $p \neq h$ ,  $h$ : harmonic number). Although this method is fairly simple to implement (for instance one can excite one of the normal RF cavities at a frequency  $(h \pm 1) f_0$ ), it reduces significantly the machine acceptance in the longitudinal plane, as some bunches see a reduced RF voltage. Similarly a large area is necessary in the transverse tune diagram to accommodate the additional bunch-to-bunch tune splitting.

Figure 6 shows an old example of longitudinal instability suppression by synchrotron frequency splitting (two different frequencies) [7].

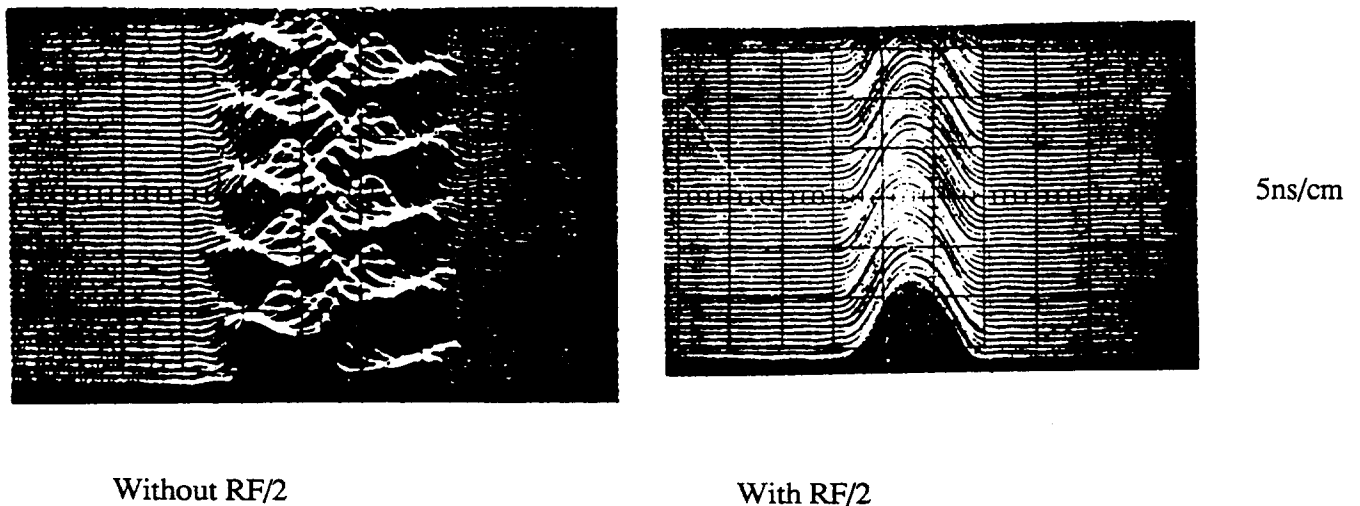


Fig. 6 Longitudinal instability in the CERN PS suppressed by frequency splitting (1970)

## 4. TRANSVERSE FEEDBACK SYSTEMS

The most effective cure against coupled bunch instabilities, transverse or longitudinal is the use of feedback systems [9]. We shall concentrate on the analysis of such systems in the following.

### 4.1 Architecture of a transverse feedback system

Figure 7 shows the schematics of a typical transverse feedback system. The beam displacement resulting from the instability is detected by pick-up electrodes, then amplified and applied as a correction to the beam with a downstream transverse deflector (or kicker).

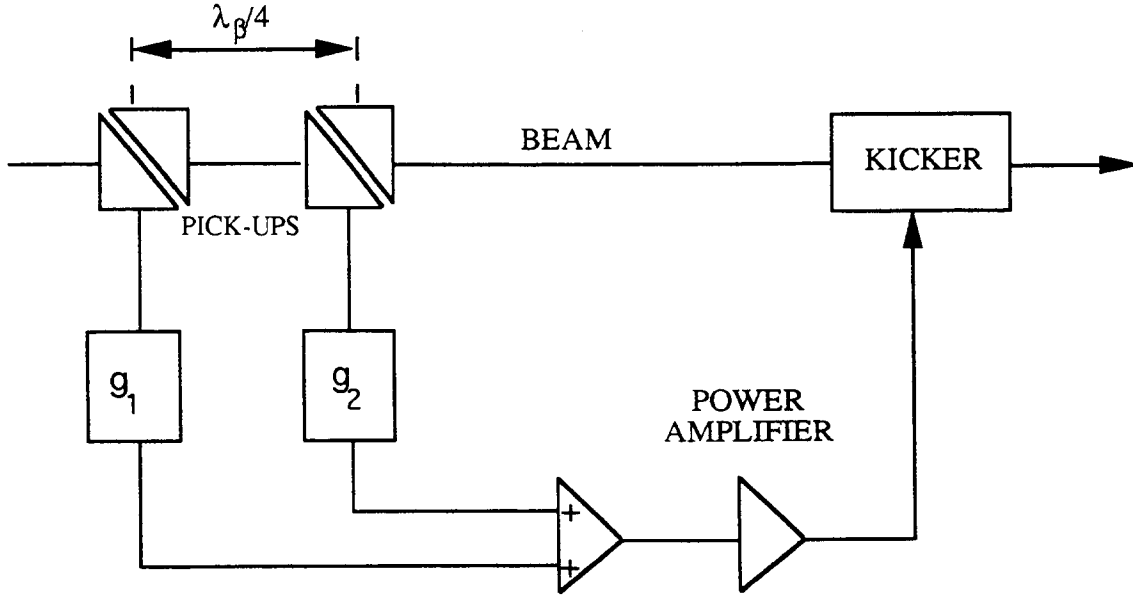


Fig. 7 A typical transverse feedback system

The transit time of the signal from pick-up electrodes to the deflector is arranged such that it matches the beam time of flight. In this way the correction is applied to the same particles which have generated the pick-up signal. To be insensitive to energy oscillations, the pick-up electrodes are better placed in a region of minimum dispersion.

Figure 8 shows the normalized transverse phase space diagram of a bunch (or ensemble of particles). Assume that the maximum displacement occurs at the pick-up location like indicated on the figure. A quarter betatron wavelength downstream, the correction is applied as a change of slope, along the  $x'$  axis. The result is a new trajectory which will spiral inwards and ultimately reach the origin.

The distance between pick-up and kicker should ideally be such that the corresponding betatron change is  $\pm 90^\circ$ . This can be achieved by combining the signals of two transverse detectors spaced by a quarter betatron wavelength (Fig. 7). For large machines (high  $Q$  values), it is easier to position pick-ups and kickers close together; in this case combining of two pick-up signals is also useful to correct for small tune changes; the overall delay is in this case close to one machine turn.

The feedback gain  $G$  is defined by the relation:

$$G = \frac{\Delta\theta}{x} \beta \quad (3)$$

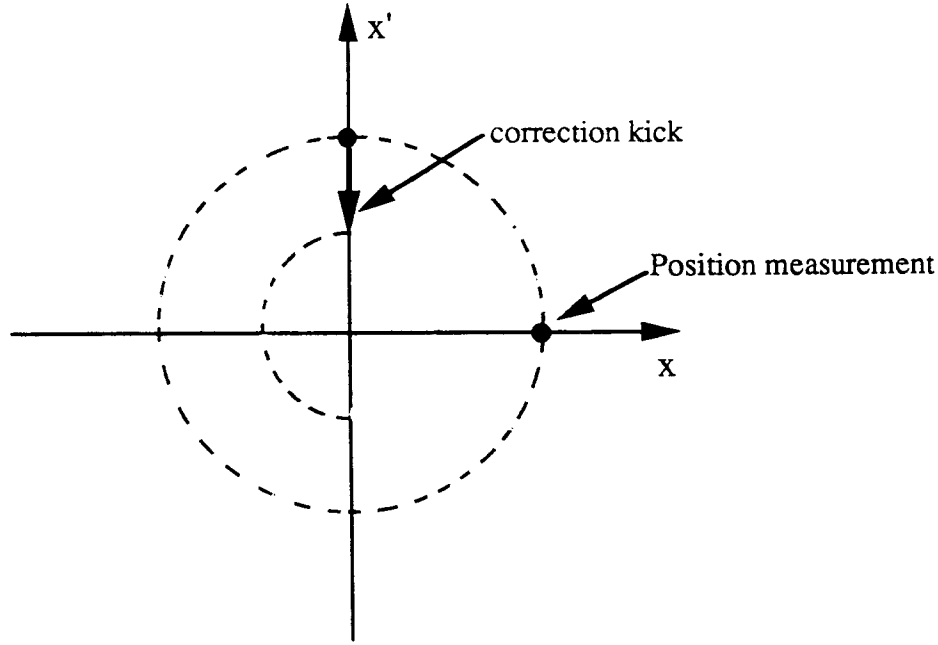


Fig. 8 Phase space diagram of a transverse bunch oscillation

where  $\Delta\theta$  is the change of slope produced by a measured displacement  $x$ , assuming the same  $\beta$  value at the pick up and at the kicker.

After one turn the displacement has been corrected by:

$$\Delta x = \beta \Delta\theta = Gx \quad (4)$$

which corresponds, per unit time (smooth approximation) to:

$$\frac{dx}{dt} = Gf_0 x \quad (5)$$

and to a damping time  $\tau = 1/Gf_0$ . This would be correct if, at each turn, the beam would pass in the detector with maximum amplitude. Obviously this is not true because the tune cannot be an integer; as a result an additional factor 1/2 comes from averaging over all possible betatron phases at the pick-up position. Finally one obtains in the ideal case (optimum pick-up - kicker phase):

$$\frac{1}{\tau} = \frac{Gf_0}{2} \quad (6)$$

If the center of gravity of each bunch has to be damped individually (ideal bunch-to-bunch damping of the dipole mode), the required bandwidth of the system is, from the Nyquist theorem,  $f_b/2$  where  $f_b$  is the bunch frequency ( $f_b = Mf_0$  for  $M$  equidistant bunches). In many cases however, the feedback gain may not be constant in the  $0 - f_b/2$  frequency interval; it can be tailored to the frequency dependent instability growth rate. In the case of the resistive-wall instability which falls off rapidly with frequency, the feedback system can be limited in bandwidth to a few revolution harmonics. It is then not necessary to measure the position of each bunch individually: averaging over several bunches or undersampling is possible.

In the case of a few unstable modes, driven by narrow-band impedances, one can also use band pass filters and treat each mode separately. This "mode-by-mode" damping offers more flexibility (phase and gain can be adjusted independently for each frequency) but becomes cumbersome for many bunches and many possible modes of instability.

## 4.2 Rejection of closed-orbit offsets – Filtering

Without any signal processing in the amplifier chain, the offset of the closed-orbit in the pick-up will be amplified by  $G$ , with two undesirable effects:

- a change of the overall closed-orbit in the machine, dependent on  $G$
- a saturation of the kicker amplifier.

To reject the unwanted closed-orbit component in the pick-up signal one discriminates between the quasi-static closed-orbit component and the fast varying betatron oscillation signal. More precisely the closed-orbit component is a periodic signal at the revolution frequency, which results from the uneven structure of the beam current along one machine turn. In particular, for a debunched beam only the DC component is present in the closed-orbit signal.

Several techniques are in use to reject the closed-orbit component of the pick-up signal. The self balanced front-end (Fig. 9) is a purely analog solution to the problem. The closed-orbit DC component (obtained after base line restitution of the pick-up signal) is used to balance the two electrodes and to bring the electrical center of the detector on the position of the closed orbit.

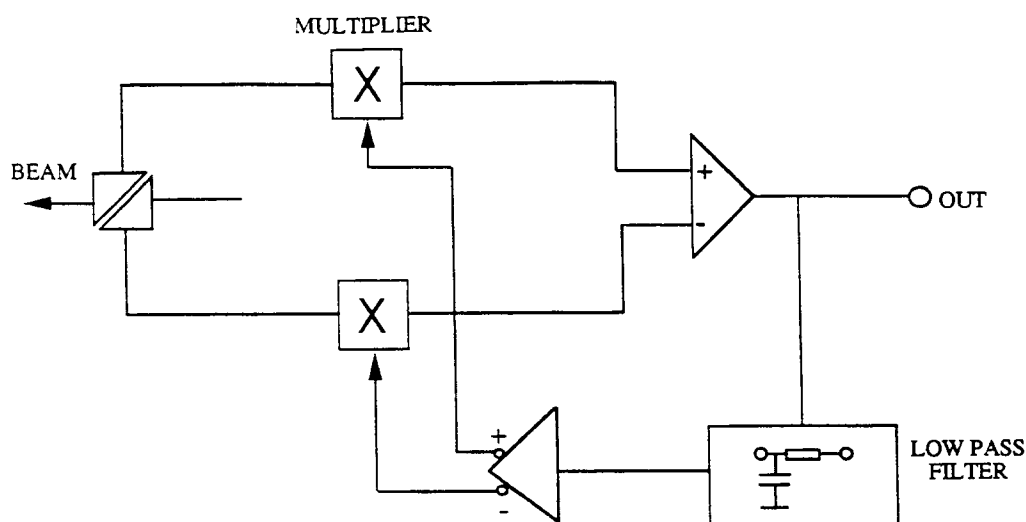


Fig. 9 Self-balanced frontend to reject closed orbit component

The more modern technique is based on periodic filters, which are conveniently constructed with digital technology. In its simplest form this filter makes the difference between the position measurements at successive turns according to the equation

$$u_n = x_n - x_{n-1} \quad (7)$$

feedback      measurement      measurement  
 signal          at turn n          at turn n-1

The closed-orbit signal being almost constant from turn to turn is rejected by the filter.

The frequency response of the filter, schematized on Fig. 10 where the position at turn  $n-1$  is obtained by a one turn delay, is simply:

$$\frac{u}{x} = 1 - \exp(-j\omega T_0) \quad (8)$$

Its amplitude and phase responses are displayed on Fig. 10. Closed-orbit signals which appear at multiples of the revolution frequency are rejected by the periodic notches (at every  $f_0$  harmonic) of the filter. The gain and **phase** of the feedback signal (whose spectral components are close to the betatron lines  $f_\beta$ ) are changed by the filter. In particular the optimum condition ( $90^\circ$  phase difference between pick-up and kicker) is no longer fulfilled.

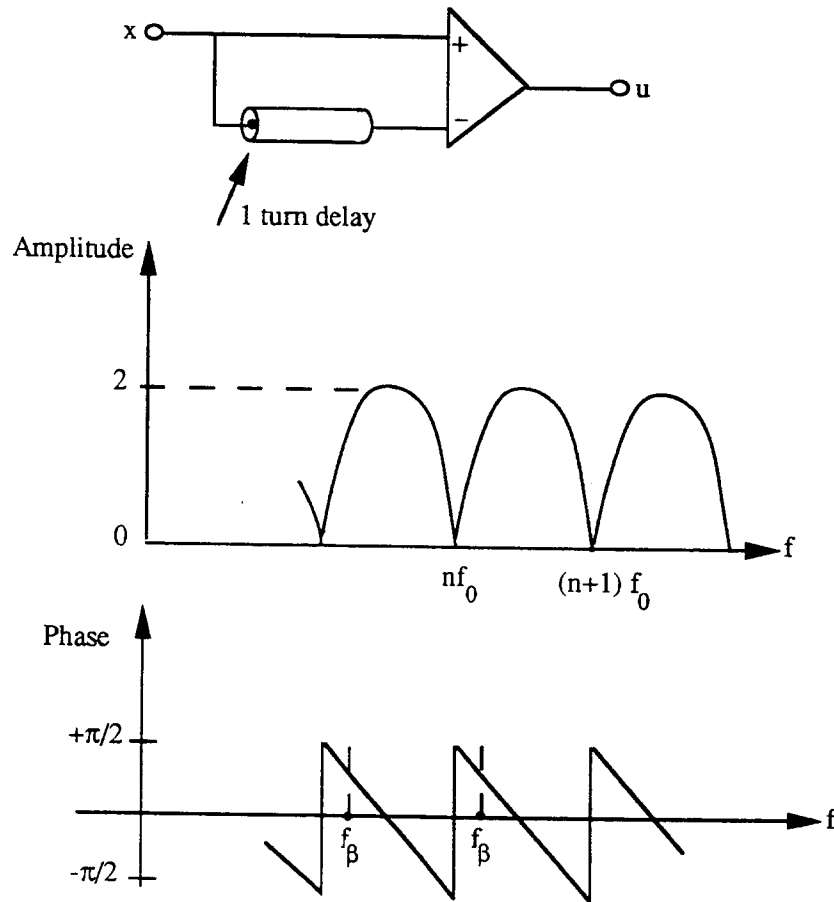


Fig. 10 Rejection of closed orbit with a single periodic filter

On the contrary, with more complicated filters, one can adjust the betatron phase to be optimum, even if the pick-up – kicker distance does not correspond to  $\pi/2$  betatron phase difference.

The architecture of the filter ensures that each bunch is treated independently of all others; this is because the memory element in the filter is exactly one turn, which means that the signal of each bunch only combines with itself, not with any other bunch signal. One can also regard the filter as being used in a time multiplexing mode (one time slot per bunch): each bunch signal is processed by the same filter elements (adder and delay), but the memory (delay) contains at a given moment the information of all bunches.

The general expression for filters having this property is given by the expression:

$$u_{m,n} = a_0 x_{m,n} + a_1 x_{m,n-1} + \dots + a_k x_{m,n-k} + b_1 u_{m,n-1} + b_2 u_{m,n-2} + \dots + b_p u_{m,n-p} \quad (9)$$

where  $m$  is the bunch number,  $n$  the turn number and  $k$  and  $p$  are integers.

The filter is **non recursive** (FIR or Finite Impulse Response) if  $b_1, b_2 \dots b_p = 0$ , otherwise it is **recursive** (IIR, or Infinite Impulse Response), according to the terminology in use in the digital filter theory. The only difference here is that, unlike a classical digital filter which is limited to the Nyquist frequency ( $f_0/2$  here), the feedback filter works beyond, because of the particular nature of the beam signal. There is no aliasing effect up to half bunch frequency  $f_b/2$  with one measurement per bunch per turn.

In other words, the filter behaves like a linear system up to  $f_b/2$ . The condition to obtain a notch filter response (zero at  $n f_0$ ) is simply:

$$\sum_{n=0}^k a_n = 0$$

The complex frequency response of the filter is given by:

$$H(j\omega) = \frac{\sum_{n=0}^k a_n \exp(-jn\omega T_0)}{1 - \sum_{n=1}^p b_n \exp(-jn\omega T_0)} \quad (10)$$

as illustrated on Fig. 11. This is characteristic of an ideal **bunch to bunch** feedback system for which all bunches are damped independently, each with the same damping rate. It also corresponds to a constant feedback gain for each betatron line.

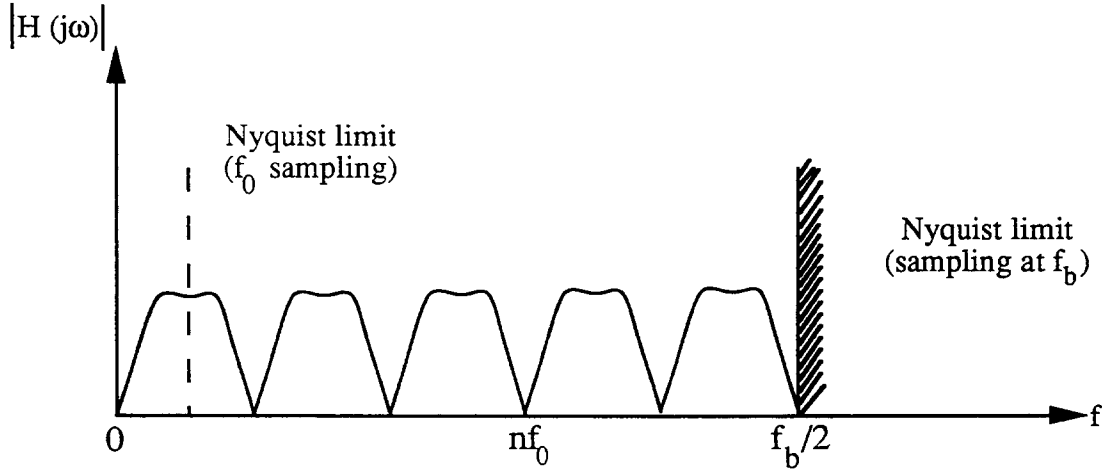


Fig. 11 Amplitude response of a periodic notch filter for a transverse feedback

In most cases however the overall feedback gain  $G$  does not need to be constant in the  $0 = f_b/2$  frequency interval. It can be tailored to the behaviour of the instability growth rate versus frequency. In particular this is the case for the resistive-wall instability, which is peaked at low frequency (Fig. 12). If the maximum frequency of interest  $f_{\max}$  is much smaller than  $f_b/2$ , sampling the position of every bunch is no longer necessary: one can

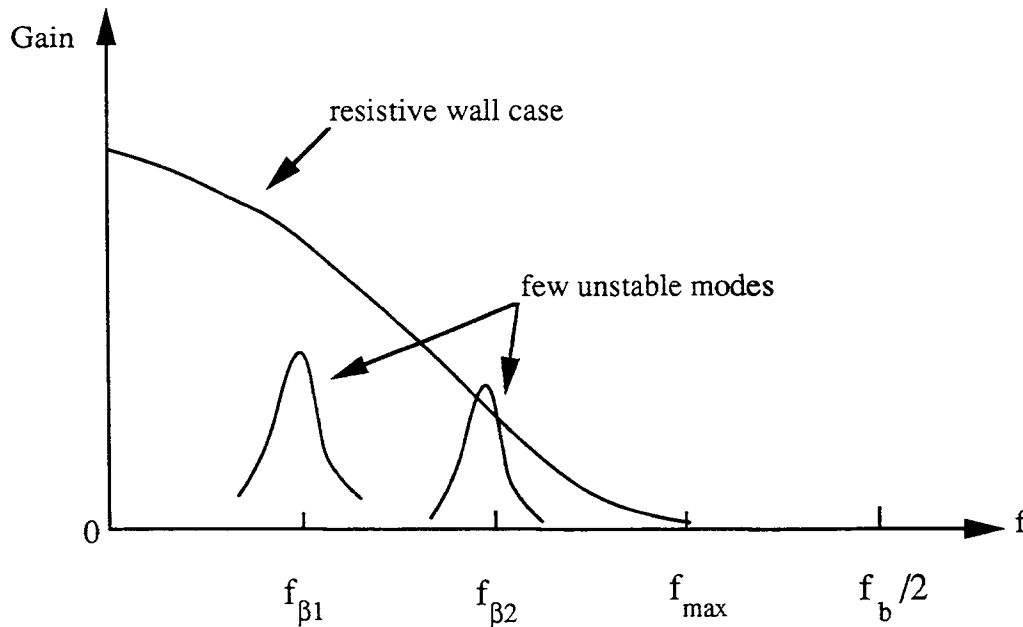


Fig. 12 Feedback gain tailored to instability characteristic

average the position measurements over several bunches (front-end bandwidth limitation) or (and) use undersampling.

When there are only a few unstable modes driven by narrow-band impedances, it may be sufficient to use selective filtering (Fig. 12). If the latter becomes very narrow to cover only one mode (filter bandwidth  $< f_0/2$ ), the feedback technique is referred to as "mode-by-mode" damping.

As explained before the **one turn delay line** is the basic building block of the transverse feedback systems. At a fixed revolution frequency  $f_0$ , analog delay lines can be used, with the benefit of simplicity. However, the product delay-bandwidth of the line rapidly becomes a limitation, especially for large machines with many bunches. Sampled filters (at  $f_b$ ) and in particular the family of  $M$  path filters can provide the desired transfer function of Fig. 11 (ideal bunch-to-bunch feedback system). Subsequent analog filtering (including the kicker frequency response) may be needed to obtain the overall gain vs. frequency curve. Analog filters with quasi constant delay (linear phase shift) are better suited to keep the phase of each betatron line close to its optimum value.

The rapid advances in digital filter technology have made this technique increasingly popular in constructing the filters of transverse feedback systems. The basic clock frequency must be a multiple of  $f_0$  (up to  $f_b$ ), which ensures delays of exactly one turn. The delay element itself is a memory, or shift register, the so-called FIFO (First In – First Out) version being the exact digital replica of an analog delay.

Sampling and digitizing at  $f_b$  is generally the most critical part of the filter from the point of view of speed ( $f_b$  can be as high as several hundred MHz) and number of bits. The latter must be compatible with the closed-orbit offset in addition to the betatron signal; it must also not introduce an unacceptable level of quantization noise. There is generally a trade off between the memory capacity and the arithmetic complexity of the processor (number of adders, multipliers, etc...). FIR filters usually need more memory capacity than their IIR counterparts for similar transfer functions. The filters with fixed parameters ( $a_n$ ,  $b_n$  coefficients) can be synthesized in a simple way (shift of binary words) if  $a_n$ ,  $b_n$  can be approximated with  $2^p$  or  $1-2^p$  ( $p$  integer).

Changes of  $f_0$  are automatically accounted for in a digital filter clocked at  $mf_0$ , except for the unavoidable fixed part of the pick-up – kicker delay (cables, analog filter, kicker delay). Compensation of fixed delays in the chain against a change of  $f_0$  is possible if the input (ADC) and output (DAC) clocks are connected to the  $mf_0$  source with different delays [10]. The difference should be equal to the fixed delay to be compensated.

### 4.3 Power requirements

Pick-ups and kickers are basically the same electromagnetic devices. They interact with the beam through the longitudinal component of their electric field [11] (Panofsky Wenzel Theorem).

A very common example considers the strip line pick-up and its kicker counterpart (Fig. 13), composed of two matched transmission lines (length  $l$ , spacing  $d$ , width  $w$ ).

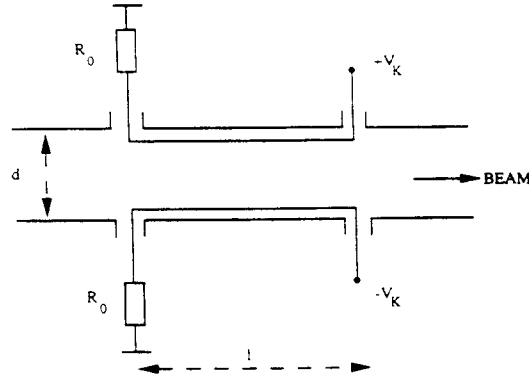


Fig. 13 Strip-line kicker

The kicker sensitivity is defined by:

$$K_{\perp} = \frac{1}{V_k} \frac{v}{e} \Delta p_{\perp} \quad (11)$$

where  $V_k$  is the applied voltage,  $v$  the particle's velocity,  $e$  the electronic charge and  $\Delta p_{\perp}$  the transverse kick impressed on the beam.

The single passage beam deflexion  $\Delta\theta$  (Eq. 3) is related to the kicker sensitivity by the relation:

$$\Delta\theta = \frac{\Delta p_{\perp}}{p} = \frac{K_{\perp} V_k e}{E \beta^2} \quad (12)$$

From the reciprocity and Panofsky Wenzel theorems one can derive the following relation between pick-up and kicker sensitivities, for the same device:

$$K_{\perp} = 2 \frac{V S_{\Delta}}{\omega R_0} \quad (13)$$

in which  $S_{\Delta}$  is the pick-up sensitivity and  $R_0$  the characteristic impedance of the line. The sensitivity of the strip line kicker of Fig. 13 is given by:

$$K_{\perp} = 2 \frac{1}{d} \underbrace{\tanh\left(\frac{\pi w}{d}\right)}_{\text{geometry factor}} \underbrace{\frac{\sin(2\pi l / \lambda)}{2\pi l / \lambda}}_{\text{frequency response}} \quad (14)$$

For a given kicker cross section, sensitivity and bandwidth depend on the length  $l$  in opposite ways. This limits the operating frequency of the kicker to about  $c/4l$ .

Strip-line kickers can also operate in an RF band (from  $mf_b$  to  $(m + \frac{1}{2})f_b$ ) using the "meander" technique [12]. Each section is  $\lambda / 4$  long (at the center frequency  $m f_b$ ), and is rotated by  $180^\circ$  along the beam axis with respect to its neighbours.

At low frequencies ( $f_b \ll c / 2l$ ) magnetic or electrostatic deflectors can be used as well. The sensitivity of the electrostatic kicker is given by:

$$\Delta\theta = V_K \frac{1}{d} \frac{e}{E\beta^2} \quad (15)$$

When driven through a tetrode  $V_K$  becomes limited at high frequencies by the maximum current of the tube (loaded by the electrode capacitance). As a result the deflexion capability decreases with frequency as in the strip line case.

In most cases the kicker power is determined by the injection transients multiplied by the feedback gain. The latter is imposed by the specified damping rate needed to suppress the instability, or to avoid undesired blow-up in case of filamentation. Random injection errors come from fluctuations in beam steering or in magnetic elements in the machine. Systematic errors may be due to uncorrected closed-orbit which cannot be rejected instantaneously by the feedback notch filter. During its setting time closed-orbit error may dominate and ultimately determine the kicker power, unless  $G$  can be reduced during this limited period of time.

Linear operation of the transverse feedback system is not necessary during injection transient damping. The fastest damping rate, for a given kicker power is achieved in saturation (bang-bang) mode [13]. In this case digital limiters provide the best performance.

In a system where maximum deflexion can only be provided at low frequencies (slew rate limited), it is important to process the beam signal in such a way as to avoid any large high frequency components which are non significant [14]. This is the case in particular when a new batch is injected with some error, after a long gap in the bunch train: special signal processors may be used to take advantage of the gap length to reduce the required rate of change of the kicker voltage.

#### 4.4 Emittance blow-up from damper noise

The noise present in the electronics of the beam detector will be amplified and applied to the beam by the transverse feedback system. One expects a coherent effect on the beam (corrected to some extent by the feedback system itself) and an incoherent one leading to beam blow-up. This is a crucial issue in colliders where small emittances are needed for high luminosity.

The overall damper configuration, including detector noise, is the same as that of a transverse cooling system, and therefore under some not too restrictive assumptions (debunched beam theory applied to a bunched beam, tune spread dominated by beam-beam effect, no loss of Landau damping) the classical cooling formula can be applied [15] [16]:

$$\frac{1}{\tau_{x^2}} = \frac{1}{2} \frac{f_0}{N} \sum_n \left[ 2 \frac{g_n}{1+S_n} - M_n \frac{g_n^2}{(1+S_n)^2} - \frac{U_n g_n^2}{(1+S_n)^2} \right] \quad (16)$$

where  $1/\tau_{x^2}$  is the growth rate of the beam emittance,  $N$  the total number of particles,  $g_n$  the feedback gain for band  $n$ ,  $M_n$  the mixing factor,  $S_n$  the feedback via the beam factor and  $U_n$  the noise /Schottky signal ratio, for full mixing. The first two terms of the right side correspond to the cooling and mixing effects, which can be shown to be negligible in the case of a transverse damper. Only remains the last term, for which  $U_n$  can be expressed as the sum of the detector noise and the external excitation (to be suppressed by the damper). One obtains:

$$\frac{1}{\tau_{x^2}} = -f_0 \sum_{n=0}^j \frac{\left( \frac{\alpha^2 g_n^2}{12j} + r_n^2 \right)}{\left( 1 + \frac{g_n}{4\delta Q} \right)^2} \quad (17)$$

where  $\alpha$  is the ratio of the Last Significant Bit of the ADC to the r.m.s beam size (the detector noise is assumed to be due to quantization in the ADC, and is assumed also to be additive),  $r_n$  is the external excitation in band  $n$ ,  $W = jf_0$  is the total bandwidth of the feedback and  $\delta Q$  the beam-beam tune spread.

The family of curves of Fig. 14 show the effect of  $g_n$  (feedback gain) in various cases. The term  $g_n/4\delta Q$  must normally be larger than unity to achieve a damping time significantly shorter than the decoherence time, and avoid blow-up. For high gains the blow-up rate only depends on detector noise, as expected. At lower gains the blow-up rate is either smaller in case detector noise dominates over external excitation, or higher in the opposite situation, (which should be the normal operating mode of the damper during coast).

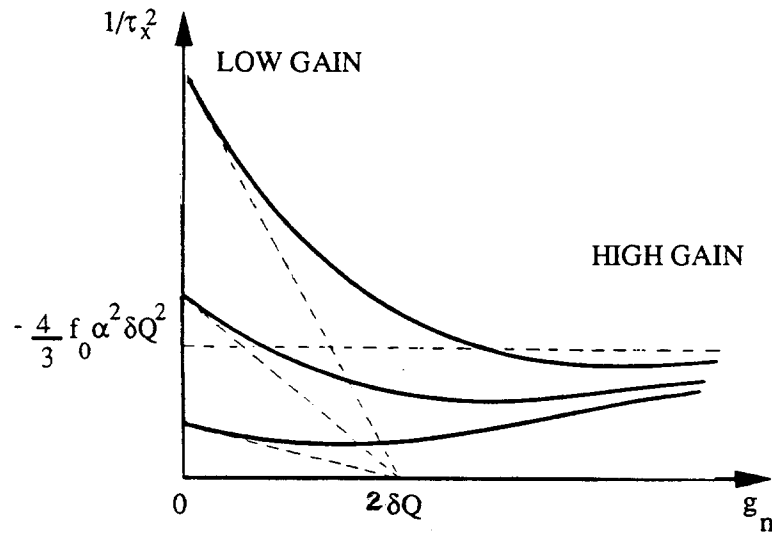


Fig. 14 Growth rate of the beam emittance due to feedback noise

## 5. LONGITUDINAL FEEDBACK SYSTEMS

### 5.1 Architecture of a longitudinal feedback system

A very simple longitudinal feedback system is sketched on Fig. 15 [7]. The radial detector is located at a position of large dispersion, such that any energy error can be easily detected and applied back to the same bunch via a longitudinal kicker. No phase shift is necessary here as the same variable (the energy deviation) is measured by the detector and applied to the beam by the kicker. The beam and signal transit times from pick-up to kicker should be identical, but, contrary to the transverse case, the distance pick-up to kicker is unimportant, because the "synchrotron wavelength" is much longer than one turn ( $Q_s \ll 1$ ).

With two radial detectors located half a betatron wavelength apart one can reduce the undesired effect of betatron oscillations and closed-orbit error. Nevertheless, the sensitivity of the energy measurement via the beam radial position cannot be very high and hence noise contamination limits severely the performance of such a system.

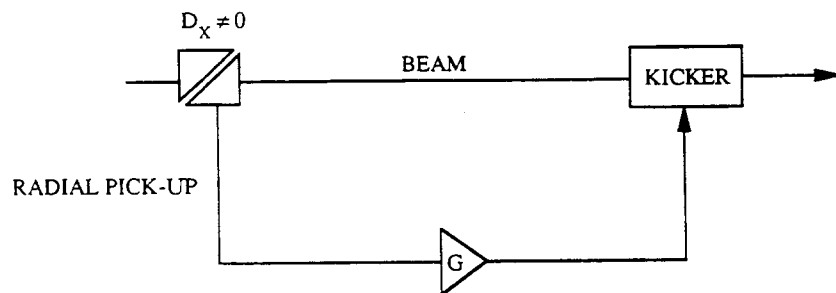


Fig. 15 A single longitudinal feedback system

Instead of a radial measurement one can use a phase measurement to detect any longitudinal oscillation of the beam. This however requires a phase shift of  $90^\circ$  at the synchrotron frequency  $f_s$  which can only be obtained by filtering, contrary to the transverse case. This is again because  $Q_s$  is much smaller than unity.

A "bunch-by-bunch" damping system is sketched in Fig. 16. The phase error signal, from a fast phase detector, is demultiplexed into  $M$  channels corresponding to  $M$  bunches. Each bunch signal is processed independently at low frequency (up to  $f_0/2$ ) such as to provide a  $90^\circ$  phase shift at the synchrotron frequency. The  $M$  signals are then multiplexed into a common kicker drive signal.

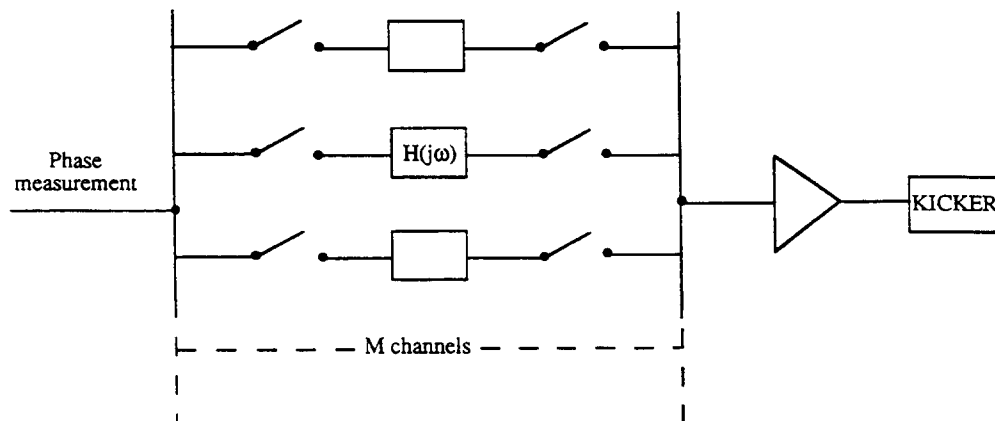


Fig. 16 Longitudinal bunch by bunch damping system

Each individual channel should have a filter characteristic  $H(j\omega)$  which not only provides high gain and  $90^\circ$  phase shift at  $f_s$ , but also negligible gain at zero frequency and  $f_0/2$ . The overall response of the " $M$  path filter", including multiplexing and demultiplexing is periodic at  $f_0$ , each half band being the replica of the  $H(j\omega)$  transfer function (Fig. 17). The system is linear (no aliasing effects) up to  $f_0/2$ . As shown in Fig. 17 feedback gain is provided at the frequencies  $nf_0 \pm f_s$  of all possible instability modes. Again there is complete equivalence between a bunch by bunch feedback system as depicted on Fig. 16 and a "mode-by-mode" feedback system with a constant gain for all instability modes.

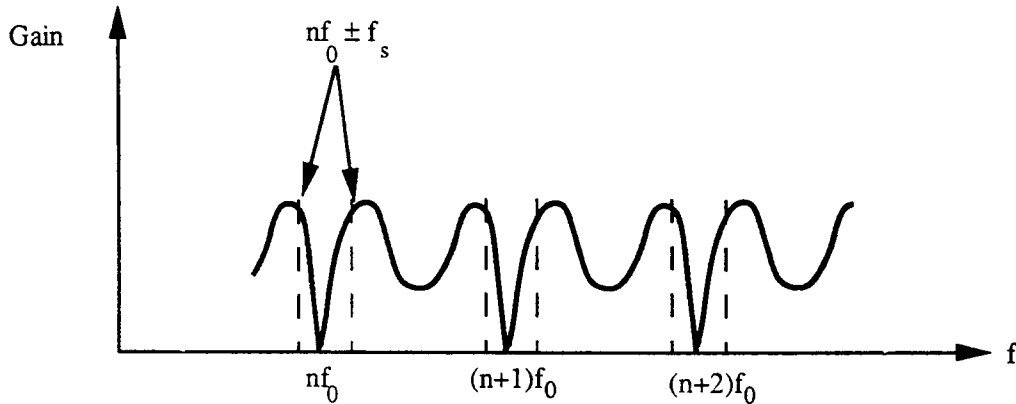


Fig. 17 Overall response of a longitudinal feedback system

## 5.2 Filtering

Periodic filters can be realized in analog technology ( $M$  path filters, Fig. 16) when the number of bunches is small. Modern digital technology is better suited in the case of many bunches. To obtain the required phase shift at  $f_s$  ( $f_s \ll f_0$ ), one needs a large delay, or in digital technology a large memory capacity for a given sampling frequency (usually  $f_0$  per bunch). On the other hand, sampling at  $f_0$  may be redundant if  $Q_s$  is very small, opening the possibility of downsampling [17] (the sampling frequency being a submultiple of  $f_0$ , per bunch). This however increases the noise in the system.

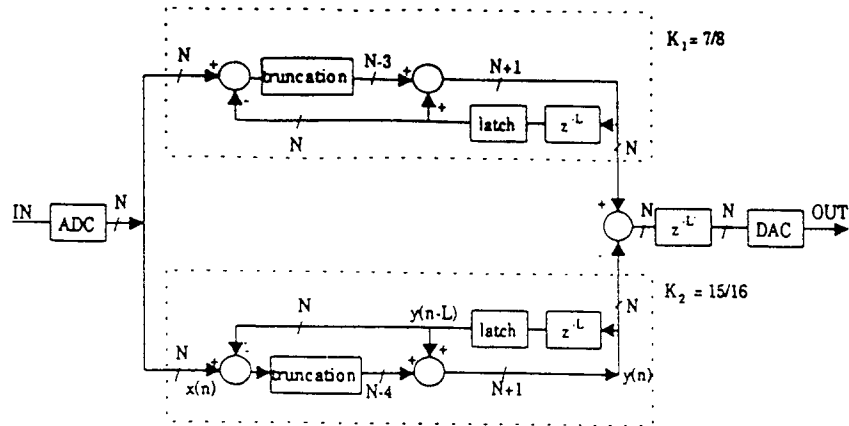
Non-recursive filters based on the difference of two phase measurements of the same bunch distant by  $m$  turns automatically provide notches at  $f_0$  harmonics (rejection of constant or slowly varying phase offsets) [18] [19]. If  $m$  is small ( $m \gg 1/Q_s$ ), the peak of  $|H(j\omega)|$  happens at a frequency much smaller than  $f_s$ . This type of operation, sometimes referred to as the "differentiator mode" provides a phase shift close to  $90^\circ$  at  $f_s$  with a small memory capacity, but at the expense of more noise coming from the unnecessarily large gain at frequencies higher than  $f_s$ . The typical duration of the transient response of the filter is given by the inverse of the peak frequency, and can be made short if necessary. This is typically the case if the feedback must quickly damp injection oscillations.

By selecting  $m = 1/2Q_s$ , the peak of  $|H(j\omega)|$  coincides with  $f_s$ , which is the best situation as far as noise is concerned. In this "peak gain mode", the  $90^\circ$  phase shift must be provided by an additional delay of length  $T_s/4$ . The total memory capacity needed thus corresponds to a total delay of  $3T_s/4$ , which is also the duration of the transient response of the filter.

Another technique, based on the difference of two recursive filters suppresses the undesirable lobes of  $|H(j\omega)|$  which appear with non recursive filters. The transfer function:

$$H(j\omega) = \frac{1 - K_1}{1 - K_1 \exp(-j\omega T_0)} - \frac{1 - K_2}{1 - K_2 \exp(-j\omega T_0)} \quad (18)$$

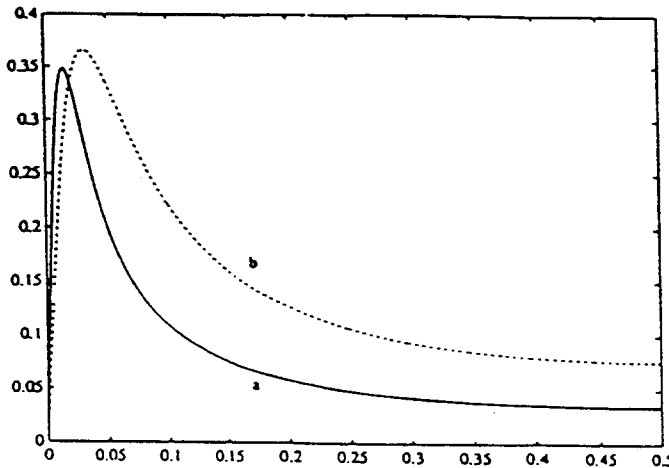
can be adjusted with two parameters  $K_1$  and  $K_2$ . In the architecture of Fig. 18  $K_1$  and  $K_2$  are of the form  $1-2^{-P}$  and multiplication can be synthesized by adding and truncation, which makes processing very fast and cheap. The frequency and transient responses of this filter are given in Fig. 18.



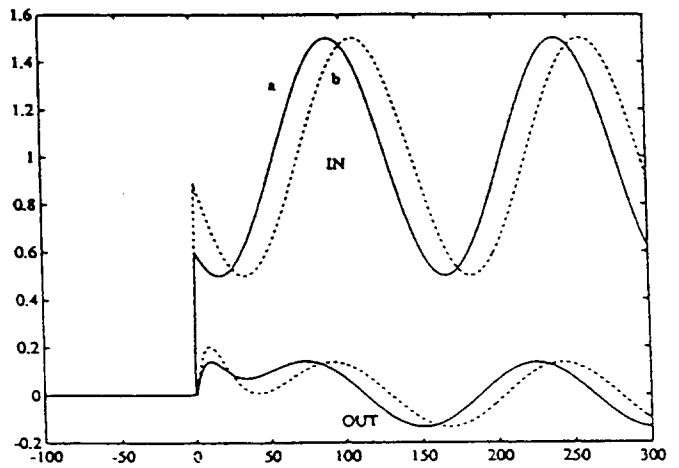
$z^{-L}$ : delay of  $L$  clock periods (one turn)  
 $z^{-L'}$ : delay of  $L'$  clock periods (one turn minus a fixed delay)  
 $N$ : number of bits

Equation of the branch of the filter with  $K=15/16$ :  
 $y(n) = y(n-L) + (x(n) - y(n-L))/16$  or  
 $y(n) = 15/16 \cdot y(n-L) + x(n)/16$

#### Architecture of the filter



Amplitude response of the filter  
a:  $K_1=7/8$ ,  $K_2=15/16$   
b:  $K_1=3/5$ ,  $K_2=7/8$



Rejection of injection offset  
top:  $f_s$  oscillation (2 phases a, b) superimposed on unit step offset  
bottom: filter output

Fig. 18 A simple longitudinal filter based on the difference of two recursive filters

### 5.3 Synthesis of a longitudinal impedance

A longitudinal dipole, coupled bunch instability is driven (above transition) by an impedance which has the property:

$$\text{Re } Z(kf_0 + f_s) > \text{Re } Z(kf_0 - f_s) \quad (19)$$

Conversely, the instability mode number  $n$  can be damped if an impedance with the opposite property:

$$\text{Re } Z(pf_b + nf_0 + f_s) < \text{Re } Z(pf_b + nf_0 - f_s) \quad (20)$$

is inserted in the beam. To avoid strong interaction with the revolution frequency line at  $pf_b + nf_0$ , one imposes the additional condition:

$$Z(pf_b + nf_0) \approx 0$$

which leads to the design objective:

$$\text{Re } Z(pf_b + nf_0 + f_s) \approx -\text{Re } Z(pf_b + nf_0 - f_s) \quad (21)$$

It can be shown that damping of quadrupole, sextupole modes can be achieved as well if the real part of the impedance is symmetric around  $pf_b + nf_0$ , over a band  $\pm 2f_s, \pm 3f_s$  respectively.

The problem here is to synthesize an impedance such that its real part changes sign every  $f_0$  harmonic to damp all possible instability modes. With a broadband detector and kicker (bandwidth  $\approx f_b$ ) the problem can be solved with periodic filters similar to those described earlier. The difference here is that the beam current signal is directly filtered (without phase detection) and transmitted to the longitudinal kicker.

The system being intrinsically sensitive to all internal bunch modes (dipole, quadrupole, etc ...) the shape of the filter in a  $0-f_0/2$  interval is important. In particular due to the unavoidable one turn delay,  $\text{Re } Z$  usually changes sign not only at  $nf_0$ , but also between  $nf_0$  and  $(n + \frac{1}{2})f_0$  making high internal bunch modes potentially unstable. These modes are however generally strongly Landau damped.

The periodic filters which cover a frequency band of width 0 to  $f_b$  are translated in frequency by coherent mixing (Fig. 19) to keep the system linear (no aliasing). The mixers (input and output, in-phase and in-quadrature), whose reference frequency is a multiple of  $f_b$  can be regarded as phase and amplitude detectors (input mixers) and phase and amplitude modulators (output mixers). In this respect the architecture of the synthesized impedance looks like a combined dipole (phase detector – phase modulator) and quadrupole (amplitude detector – amplitude modulator) longitudinal damper, with the two periodic filters attributed to each bunch mode (dipole and quadrupole).

### 5.4 Pick-ups and kickers

Longitudinal beam detectors are straightforward devices, with large bandwidth and dynamic range. In the case of closely spaced bunches the problem of independent phase measurement of each bunch needs special treatment. The bunch signal is transformed into an RF burst of finite duration (ideally), which is shorter than the bunch to bunch distance. This signal is used to make the phase comparison with a reference frequency at a multiple of  $f_b$ .

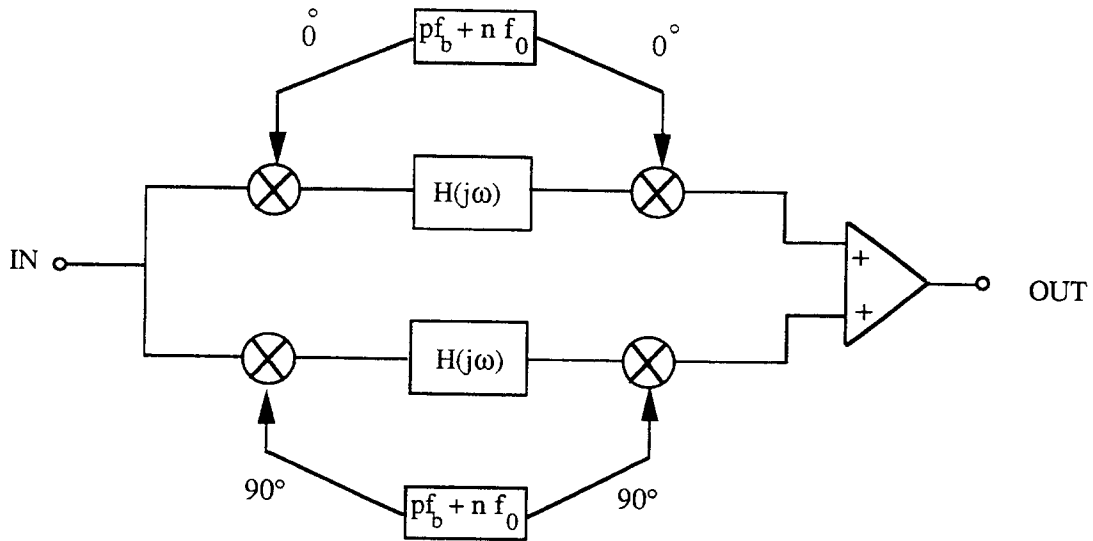


Fig. 19 Coherent mixing (in phase and quadrature) for frequency translation

The RF burst generation can be made directly by combining the signals of several pick-up electrodes located at wavelengths intervals or with an array of directional couplers. A typical output of the RF burst generator developed for the SLAC B factory is given on Fig. 20.

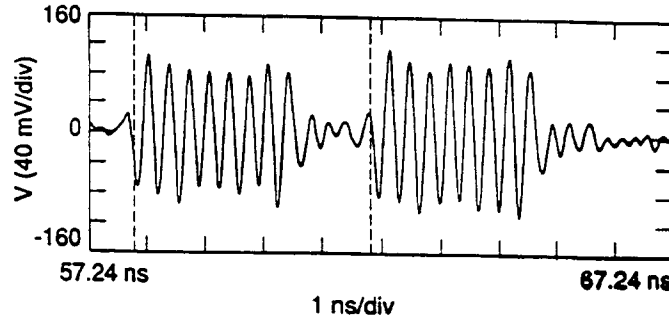


Fig. 20 Independent phase measurement of closely spaced bunches: PEP-II burst generator output

The feedback voltage  $V_f$  applied to the beam is determined by the required gain (or damping time  $\tau_f$ ) and the initial phase error, according to:

$$V_f = 2 \frac{\Delta\omega_s}{\omega_s} V \cos \phi_s \Delta\phi \quad (22)$$

where  $\Delta\omega_s = 1/\tau_f$ ,  $\omega_s = 2\pi f_s$ ,  $V$ : RF voltage,  $\phi_s$ : stable phase angle and  $\Delta\phi$ : initial phase error.

The initial phase error is usually large if the feedback system must damp injection oscillations (this is typically the case for proton machines), whereas  $\Delta\phi$  can be chosen not much above the detection threshold of the phase measurement in case the feedback system only prevents instabilities from developing.

The RF cavities can be used as longitudinal kickers if their bandwidth is large enough. The feedback voltage appears there on the skirts of the resonance curve of the cavity, whose transfer function must be properly accounted for by filtering. This technique is used in the CERN PS Booster, and is particularly well suited there because of the large frequency sweep

during acceleration. Dedicated feedback cavities are also considered, for instance for LHC, with a flattened frequency response provided by RF feedback.

With short bunches, as in  $e^+e^-$  machines, very high frequency kickers or cavities [21] are interesting because of their small size. The travelling wave kicker for the SLAC B factory [1] is composed of an array of gaps connected in series with half wavelength lines (radial and azimuthal) (Fig. 21).

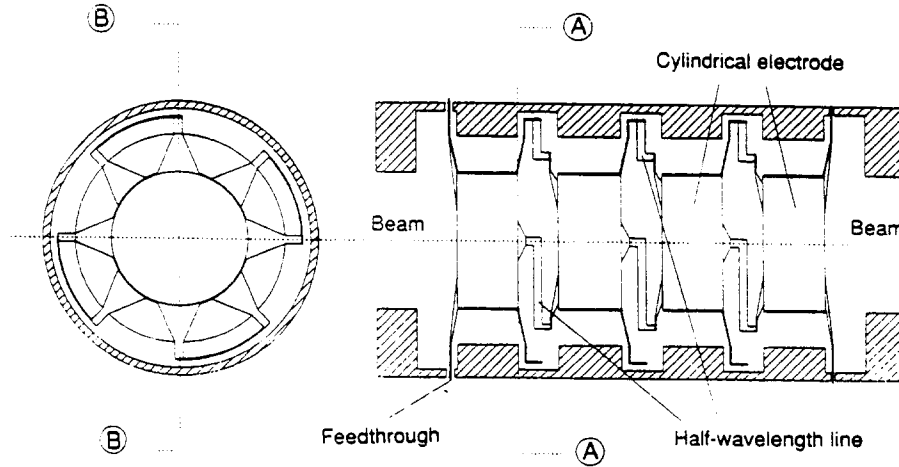


Fig. 21 Travelling wave longitudinal kicker for the SLAC B factory

### 5.5 Instabilities driven by the fundamental mode of RF cavities

In this particular case, the availability of an already existing kicker, namely the RF cavity and its associated power amplifier calls for a special treatment of the problem.

The stability of the  $n = 0$  mode is governed by the well known Robinson stability criterion, valid without loops. It sets limits on the detuning angle and maximum current. In the presence of loops (e.g. tuning loop, amplitude loop, etc ...) the stability criterion is strongly perturbed and in general difficult to evaluate precisely. The RF feedback technique is often used in this case to dramatically increase the stability margin.

For large rings ( $f_0$  small), the cavity detuning may exceed  $f_0$ . This is the case if:

$$\frac{1}{2} \frac{R}{Q} f_{RF} \frac{I_b}{V} \geq f_0 \quad (23)$$

where  $R/Q$  is the cavity geometric parameter and  $I_b$  the RF component of the beam current. In this case mode  $n = 1$  ( $f_0$  away from  $f_{RF}$ ) can sit on the cavity resonance and be strongly excited. A possible cure is with RF feedback to reduce the cavity dynamic impedance to an acceptable value. This is limited, however by the RF amplifier delay and peak power capability of the tube, which must compensate the  $n = 1$  component at  $I_b$  [21].

Another type of approach is to limit cavity detuning below  $f_0$ , by using cavities having a parameter  $\frac{R}{Q} \cdot \frac{1}{V}$  small. This parameter is inversely proportional to the charge stored on the equivalent cavity capacitor. It can be reduced by at least one order of magnitude using large aperture superconducting cavities, as compared to conventional copper structures. Another solution is with storage cavities outside the beam line and coupled to the accelerating cavity; in this case however new resonant modes appear, which must be properly corrected [23].

## REFERENCES

- [1] An asymmetric B factory based on PEP - SLAC 372, Feb. 1991.
- [2] R. Boni, A. Gallo, Status of the DAFNE RF system, 4th European Part. Acc. Conf., EPAC 94, London.
- [3] H. Padamsee et al., Accelerating cavity development for the Cornell B factory CESR B, 1991 Part. Acc. Conf., San Francisco, p. 786-788.
- [4] R. Boni et al., Update on the broadband waveguide to  $50\Omega$  coaxial transition for parasitic mode damping in the DAFNE RF cavities, 4th EPAC, London June 1994.
- [5] W.R. Smythe et al., A versatile RF cavity mode damper, EPAC 1990, Nice, p. 976-978.
- [6] F. Sacherer, A longitudinal stability criterion for bunched beam, 1973, Part. Acc. Conf., p. 825.
- [7] D. Boussard, J. Gareyte, Damping of the longitudinal instability in the CERN PS, Proc. 8th International Conf. of High Energy Accelerator, CERN 1971.
- [8] J.M. Baillod et al., A second harmonic (6-16 MHz) RF system with feedback reduced gap impedance for accelerating flat topped bunches in the CERN PS booster, IEEE Trans. Nucl. Science, NS30 n°4, Aug. 1983, p. 3499.
- [9] F. Pedersen, Feedback systems, CERN PS/90-49 (AR).
- [10] D. Boussard, G. Lambert, Reduction of the apparent impedance of wideband accelerating cavities by RF feedback, PAC 1983, Sante Fe, and CERN SPS/83-18.
- [11] D. Boussard, Schottky noise and beam transfer function diagnostics, CERN Accelerator School, Oxford 1985, CERN 87-03.
- [12] I.N. Ivanov, V.A. Melnikov, A.S. Scheulin, The meander kickers for the transverse damping system of the cycle accelerators, JINR, Dubna 1993.
- [13] R. Bossart, R. Louwerse, J. Mourier, L. Vos, Operation of the transverse feedback system at the CERN SPS, Part. Acc. Conf. Washington DC, 1987, p.763-765.
- [14] D. Boussard, E. Onillon, Damping of phase errors at injection in the LHC, IEEE, Trans. Nucl. Science, NS-40 (1993), p. 2379-2381.
- [15] D. Boussard, Evaluation of transverse emittance growth from damper noise in the collider, CERN SL/Note 92-79 (RFS).
- [16] W. Chou, J. Peterson, The SCC transverse feedback systems in "Supercolliders and Superdetectors", Editors W.A. Barletta, H. Leutz, World Scientific 1993.
- [17] Hindi et al., Down sampled signal processing for a B factory bunch by bunch feedback system, EPAC, Berlin, March 1992.
- [18] L. Ma, S. Kurokawa, E. Kikutani, FIR filters for the bunch by bunch feedback system of TRISTAN II, KEK Report 1993.
- [19] F. Pedersen, Multibunch feedback, Lecture Notes in Physics, 425, Springer-Verlag, Berlin (1994).

- [20] D. Briggs et al., Prompt bunch by bunch synchrotron oscillation detection via fast phase measurement, PAC, San Francisco , May 1991.
- [21] M. Ebert et al., Transverse and longitudinal multibunch feedback systems for PETRA, DESY 91-036.
- [22] D. Boussard, RF power requirements for a high intensity proton collider, CERN SL/91-16 revised.
- [23] Y. Yamazaki, T. Kagemaya, A three cavity system which suppresses the coupled bunch instability associated with the accelerating mode, KEK Preprint 93-15 (1993).